

Threshold Cusp Structures in the Presence of Isospin Symmetry Breaking

Katsuyoshi SONE¹ and Tetsuo HYODO²

¹*Department of Physics, Tokyo Metropolitan University, Hachioji 192-0397, Japan*

²*Research Center for Nuclear Physics (RCNP), Ibaraki, Osaka 567-0047, Japan*

E-mail: ¹sone-katsuyoshi@ed.tmu.ac.jp, ²hyodo@rcnp.osaka-u.ac.jp

(Received February 21, 2019)

We study the behavior of the cusp structures focusing on the isospin-breaking effects. The properties of the near-threshold exotic hadrons are encoded in the shapes of the cusp structures. In hadron scattering, it is often the case that the thresholds of isospin partner channels are located within a narrow energy region. To analyze the scattering in such systems, it is therefore essential to study the cusp structures that emerge at two closely separated thresholds with isospin symmetry breaking. In this study, we propose a practical representation of the scattering amplitude and show that the two neighboring cusp structures are related through the isospin symmetry.

KEYWORDS: Threshold cusp, Low-energy scattering, Multichannel scattering

1. Introduction

Many exotic hadrons are known to appear in the vicinity of reaction thresholds. In the low-energy region near the threshold, the scattering length is the key physical quantity governing the scattering. Since the value of the scattering length is reflected in the shape of the threshold cusp structure [1, 2], studying the behavior of threshold cusps is essential for understanding the properties of exotic hadrons [3–6].

In some two-body hadronic systems, isospin symmetry causes two reaction thresholds to lie within a few MeV region. In such situations, the associated cusp structures emerge within a narrow energy window. In this work, we study how these cusp features behave in both isospin-symmetric and isospin-breaking situations, using the ΛN - ΣN coupled-channels system as a typical example.

2. Formulation

In this work, we consider ΛN - ΣN coupled-channels scattering system, which includes three channels, Λp , $\Sigma^+ n$, and $\Sigma^0 p$ with the total charge $Q = +1$. In the isospin basis, these channels correspond to ΛN - ΣN with $I = 1/2$ and ΣN with $I = 3/2$. The system involves two spin channels, singlet $J = 0$ and triplet $J = 1$. Because ΛN - ΣN is the scattering between non-identical particles, each spin component contains both isospin $I = 1/2$ and $I = 3/2$ channels. In the following, we do not specify the spin component explicitly, and the results can be applied to either spin channel. In this system, the energy difference $\Delta_{\Sigma N} \sim 2$ MeV between the $\Sigma^+ n$ and $\Sigma^0 p$ thresholds is very small as a consequence of the isospin symmetry.

We focus on the threshold cusp structures in the Λp elastic scattering at the $\Sigma^+ n$ - $\Sigma^0 p$ thresholds. First, we construct the scattering amplitude, which is described by a 3×3 matrix in channel space. The optical theorem leads to the inverse of the scattering amplitude

$$f^{-1} = \hat{K}^{-1} - i\hat{p}, \quad (1)$$

where \hat{K} is called the K -matrix and describes the interactions between the channels. In this analysis, we employ an isospin-symmetric K -matrix with real constants C_i :

$$\hat{K} = \begin{pmatrix} C_1 & \sqrt{2}C_4 & C_4 \\ \sqrt{2}C_4 & C_2 & \sqrt{2}(C_2 - C_3) \\ C_4 & \sqrt{2}(C_2 - C_3) & C_3 \end{pmatrix}. \quad (2)$$

In a general three-channel scattering, the K -matrix contains six independent real parameters. However, the K -matrix (2) includes only four parameters due to the isospin symmetry. The imaginary part of Eq. (1) is given solely by the momenta of each channel

$$\hat{p} = \begin{pmatrix} p_{\Lambda p} & 0 & 0 \\ 0 & p_{\Sigma^+ n}(E) & 0 \\ 0 & 0 & p_{\Sigma^0 p}(E) \end{pmatrix}, \quad (3)$$

where $p_{\Lambda p}$, $p_{\Sigma^+ n}(E)$ and $p_{\Sigma^0 p}(E)$ represent the relative momenta of the Λp , $\Sigma^+ n$, and $\Sigma^0 p$ channels, respectively. We note that the momentum $p_{\Lambda p}$ is taken to be a constant, because the Λp threshold lies sufficiently far from the region near the ΣN threshold which is of our interest. The momenta $p_{\Sigma^+ n}(E)$ and $p_{\Sigma^0 p}(E)$ depend on the energy E and take different values at the same energy E because of the small threshold energy difference $\Delta_{\Sigma N}$. In the limit $\Delta_{\Sigma N} \rightarrow 0$, where the $\Sigma^+ n$ and $\Sigma^0 p$ thresholds coincide, these two momenta become identical and the scattering amplitude in Eq. (1) is reduced to an isospin-symmetric form. Therefore, the matrix \hat{p} provides the source of the isospin symmetry breaking in the scattering amplitude arising from $\Delta_{\Sigma N} \neq 0$ [6].

From Eqs. (1), (2) and (3), the Λp elastic scattering amplitude $f_{\text{el}}(E)$ near the threshold of channel i ($i = \Sigma^+ n, \Sigma^0 p$) can be written as

$$f_{\text{el}}(E) = f_0^i \frac{1 + ib_i p_i(E)}{1 + ia_i p_i(E)} \quad (i = \Sigma^+ n, \Sigma^0 p) \quad (4)$$

where a_i represents the complex scattering length of channel i . We note that $b_{\Sigma^+ n}$ is real, whereas $b_{\Sigma^0 p}$ is in general complex. The coefficients f_0^i in Eq. (4) corresponds to the scattering amplitude at the threshold of channel i . Using Eq. (4), the s -wave cross section near the threshold of channel i can be expanded in terms of the momentum $p_i(E)$ of channel i

$$\sigma_{\text{el}}(E) = 4\pi |f_0^i|^2 \left(1 + 2 \text{Im}[a_i - b_i] p_i(E) + \mathcal{O}(p_i^2(E))\right), \quad (\text{above the threshold}), \quad (5)$$

$$\sigma_{\text{el}}(E) = 4\pi |f_0^i|^2 \left(1 + 2 \text{Re}[a_i - b_i] \kappa_i(E) + \mathcal{O}(\kappa_i^2(E))\right), \quad (\text{below the threshold}). \quad (6)$$

The real momentum $\kappa_i(E) \equiv -ip_i(E)$ is introduced in Eq. (6), because $p_i(E)$ becomes pure imaginary below the threshold of channel i . From Eqs. (5) and (6), one can see that the slopes of the cross section above and below the threshold of channel i are determined by a_i and b_i . It should be noted that the slopes of the cross section at the threshold go to infinity when the energy E is used as a variable. In this case, the shape of the cusp structure is determined only by the signs of the real and imaginary parts of $a_i - b_i$ [6].

To clarify the contribution of the isospin-breaking effects $\Delta_{\Sigma N}$ in the slopes of the cross section, we expand $a_{\Sigma^+ n} - b_{\Sigma^+ n}$ and $a_{\Sigma^0 p} - b_{\Sigma^0 p}$ in terms of $\sqrt{2\mu_i \Delta_{\Sigma N}}$

$$a_{\Sigma^+ n} - b_{\Sigma^+ n} \simeq 2R + X \sqrt{2\mu_{\Sigma^0 p} \Delta_{\Sigma N}} \quad (\text{at the threshold of } \Sigma^+ n), \quad (7)$$

$$a_{\Sigma^0 p} - b_{\Sigma^0 p} \simeq R + W \sqrt{2\mu_{\Sigma^+ n} \Delta_{\Sigma N}} \quad (\text{at the threshold of } \Sigma^0 p), \quad (8)$$

$$R \equiv -C_4^2 / \{ (1 - iC_1 p_{\Lambda p}) C_1 \}, \quad (9)$$

where μ_i ($i = \Sigma^+n, \Sigma^0p$) represents the reduced mass of channel i and X and W are the complex constants which are determined by the K -matrix components and the constant momentum $p_{\Lambda p}$. The second terms in Eqs. (7) and (8) vanish in the isospin-symmetric limit $\Delta_{\Sigma N} \rightarrow 0$ and therefore those terms represent the contributions of the isospin-breaking effects in the slopes of the cross section. The first terms in Eqs. (7) and (8), which do not include $\Delta_{\Sigma N}$, are identical up to the factor 2. This implies that the signs of the real and imaginary parts of $a_{\Sigma^+n} - b_{\Sigma^+n}$ and $a_{\Sigma^0p} - b_{\Sigma^0p}$ coincide with each other when the isospin-breaking effects are small: $2|R/X| \gg \sqrt{2\mu_{\Sigma^0p}\Delta_{\Sigma N}}$ and $|R/W| \gg \sqrt{2\mu_{\Sigma^+n}\Delta_{\Sigma N}}$. Consequently, it is expected that the identical types of the cusp structures appear at the thresholds of Σ^+n and Σ^0p for small isospin breaking effects.

Next, we discuss the behavior of the threshold cusp structure in the isospin-symmetric limit $\Delta_{\Sigma N} \rightarrow 0$. In this case, the thresholds of Σ^+n and Σ^0p are degenerate and only one cusp structure appears at the threshold of ΣN . In the same way as Eqs. (7) and (8), the slopes of the cross section at the threshold of ΣN is obtained as

$$a_{\Sigma N} - b_{\Sigma N} = 3R, \quad (\Delta_{\Sigma N} \rightarrow 0), \quad (10)$$

where the scattering length $a_{\Sigma N}$ and complex constant $b_{\Sigma N}$ are defined as

$$\begin{cases} a_{\Sigma N} = a_{\Sigma^+n} + a_{\Sigma^0p}, \\ b_{\Sigma N} = b_{\Sigma^+n} + b_{\Sigma^0p}, \end{cases} \quad (\Delta_{\Sigma N} \rightarrow 0). \quad (11)$$

Equations (10) and (11) show that the slopes of the cross section in the isospin-symmetric limit is given by the sum of $a_{\Sigma^+n} - b_{\Sigma^+n}$ and $a_{\Sigma^0p} - b_{\Sigma^0p}$ with $\Delta_{\Sigma N} \rightarrow 0$. From this result, we therefore conclude that the two cusp structures at the thresholds of Σ^+n and Σ^0p merge into a single cusp in the $\Delta_{\Sigma N} \rightarrow 0$ limit.

3. Numerical results

In this section, we study the behavior of the threshold cusp structures numerically, focusing on the isospin-breaking effects. In this calculation, the ΣN threshold energy is defined as the midpoint between the Σ^+n and Σ^0p thresholds, and this point is chosen as the origin of the energy. To discuss the behavior of the cusps, we focus on the s -wave cross section which is proportional to $|f_{\text{el}}(E)|^2$ in Eq. (4). In this analysis, we use a dimensionless s -wave cross section

$$\sigma_{\text{el}}(E) = \frac{|f_{\text{el}}(E)|^2}{|f_{\text{el}}(E = 0; \Delta_{\Sigma N} \rightarrow 0)|^2}, \quad (12)$$

where $f_{\text{el}}(E = 0; \Delta_{\Sigma N} \rightarrow 0)$ corresponds to the Λp elastic scattering amplitude in the isospin-symmetric limit. Accordingly, in the isospin-symmetric limit, the cross section $\sigma_{\text{el}}(E; \Delta_{\Sigma N} \rightarrow 0)$ is normalized at the threshold of channel ΣN . The hadron masses used in this calculation are taken from Ref. [7].

First, we consider a simplified model where the scattering amplitude is determined solely by the scattering length of ΣN ($a_{\Sigma N}$). We impose the conditions $C_1 C_3 - C_4^2 = 0$ and $C_2 - 2C_3 = 0$ on the parameters in Eq. (2) to make the K -matrix (2) separable. In this case, the scattering amplitude $f_{\text{el}}(E)$ corresponds to the Flatté amplitude which does not include background effects (see, e.g. Ref. [5]). Consequently, the behavior of resulting cross section is characterized only by the scattering length $a_{\Sigma N}$.

As a representative example, we set the scattering length $a_{\Sigma N}$ in Eq. (11) as a typical hadronic scale

$$a_{\Sigma N} = -1.0 - i0.8 \text{ fm}. \quad (13)$$

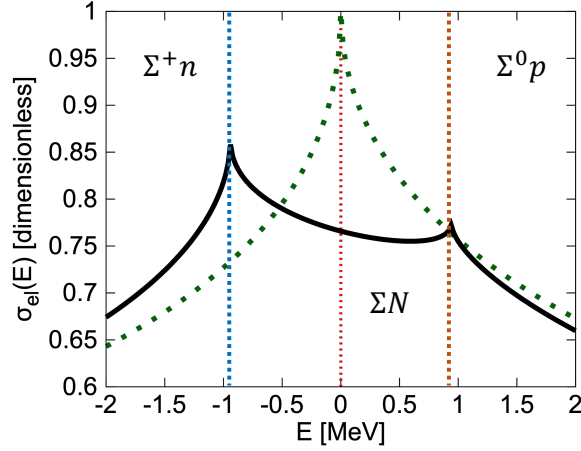


Fig. 1. The normalized Λp elastic cross section $\sigma_{\text{el}}(E)$ in Eq. (12) with the scattering length $a_{\Sigma N} = -1.0 - i0.8$ fm. The solid line corresponds to the isospin-broken cross section and the dotted line represents the isospin-symmetric one. The dotted vertical lines represent the thresholds of channel Σ^+n , ΣN and $\Sigma^0 p$.

With this scattering length, a quasivirtual pole [8] is generated below the threshold of the ΣN channel. For $a_{\Sigma N}$ in Eq. (13), the scattering lengths of Σ^+n and $\Sigma^0 p$ for the isospin broken case are calculated as

$$a_{\Sigma^+n} = -0.65 - i0.46 \text{ fm}, \quad a_{\Sigma^0 p} = -0.26 - i0.27 \text{ fm}. \quad (14)$$

The normalized cross sections in Eq. (12) are shown in Fig. 2. The cross section in the isospin-symmetric limit ($\Delta_{\Sigma N} \rightarrow 0$) is shown by the dotted line and the solid line corresponds to the isospin broken one $\sigma_{\text{el}}(E)$ with finite $\Delta_{\Sigma N}$.

As seen in the solid line in Fig. 1, the cross section $\sigma_{\text{el}}(E)$ with finite $\Delta_{\Sigma N}$ exhibits similar upward cusp structures at the Σ^+n and $\Sigma^0 p$ thresholds. Moreover, we can see that the cusp at the Σ^+n threshold is sharper than that at the $\Sigma^0 p$ threshold. This behavior can be explained by the factor 2 in Eq. (7). These results indicate that the isospin-breaking effects are small. In fact, the sum of a_{Σ^+n} and $a_{\Sigma^0 p}$ is nearly identical to the scattering length $a_{\Sigma N}$ in the isospin-symmetric limit in Eq. (13):

$$a_{\Sigma^+n} + a_{\Sigma^0 p} = -0.91 - i0.73 \approx a_{\Sigma N}. \quad (15)$$

When the isospin-breaking effect is small, the shape of the cusps is mainly determined by R in Eqs. (7), (8), and (10). Therefore, the dotted line in Fig. 1, representing the isospin symmetric limit, also exhibits an upward cusp.

Next, we calculate cusp structures in the spin-triplet ΛN - ΣN scattering with more realistic interaction. From now on, we deal with four parameters C_i independently. The spin-triplet scattering lengths are taken from the chiral EFT analysis in Refs. [9–11]. In this case, the resulting cross section corresponds only to the spin-triplet component of the elastic Λp cross section, while the physical cross section generally includes both spin-triplet and spin-singlet contributions.

In Ref. [9], the spin-triplet ΣN scattering lengths are given for the NLO19 with cutoff $\Lambda = 500$ MeV as

$$a_{1/2} = 0.95 - i4.8 \text{ fm}, \quad a_{3/2} = -0.42 \text{ fm}, \quad (16)$$

where $a_{1/2}$ is the scattering length for the total isospin $I = 1/2$ and $a_{3/2}$ is that for $I = 3/2$. Note that the state ΣN with $I = 3/2$ has no decay channels and therefore the imaginary part of $a_{3/2}$ is exactly

Table I. Spin-triplet scattering lengths of ΣN in the charge basis with Eq. (16) and $C_1 = 2.0$ fm.

Channel	Isospin symmetric (fm)	Isospin broken (fm)
$\Sigma^+ n$	$0.77 - i3.2$	$-0.48 - i3.0$
$\Sigma^0 p$	$0.6 - i1.6$	$0.52 - i0.92$

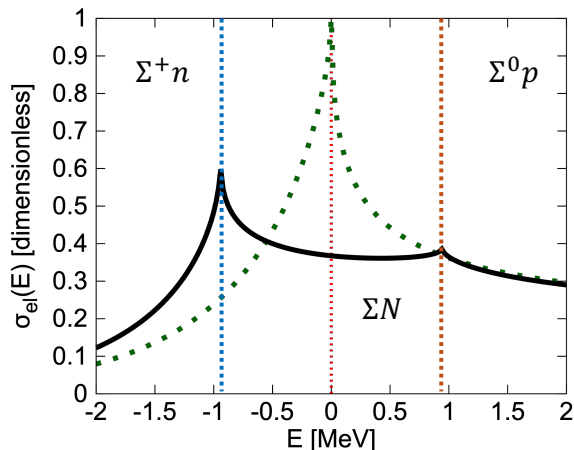


Fig. 2. Same as Fig. 1 but the scattering lengths are fixed as Eq. (16) with $C_1 = 2.0$ fm.

zero in Eq. (16). From Eq. (16), three conditions are imposed on the four parameters in Eq. (2). To determine all parameters, we fix the parameter $C_1 = 2.0$ fm. The scattering lengths in the charge basis can be obtained from those in isospin basis by using the Clebsch-Gordan decomposition for $1/2 \otimes 3/2$

$$a_{\Sigma^+ n} = \frac{1}{3}a_{3/2} + \frac{2}{3}a_{1/2}, \quad a_{\Sigma^0 p} = \frac{2}{3}a_{3/2} + \frac{1}{3}a_{1/2}. \quad (17)$$

The charge-basis scattering lengths corresponding to the chiral EFT results (16) are summarized in Table I. The corresponding Λp elastic cross sections are shown in Fig. 2.

From the solid line in Fig. 2, we can see that the cross section with finite $\Delta_{\Sigma N}$ shows the upward cusp structures at both of the $\Sigma^+ n$ and $\Sigma^0 p$ thresholds. The dotted line in Fig. 2, corresponding to the isospin-symmetric case, also shows the upward cusp at the ΣN threshold. These qualitative features, namely the appearance of upward cusp structures at the thresholds, are similar to those observed in Fig. 1. On the other hand, the difference in the sharpness of the cusp structures at the $\Sigma^+ n$ and $\Sigma^0 p$ thresholds is much more pronounced than that in Fig. 1. Although a mild asymmetry is already present in Fig. 1, it is strongly enhanced in Fig. 2, where the $\Sigma^+ n$ cusp becomes much more pronounced while the $\Sigma^0 p$ cusp is strongly suppressed. Such a strong asymmetry in the sharpness of the $\Sigma^+ n$ and $\Sigma^0 p$ cusp structures is attributed to the effects of isospin breaking. In fact, the sum of the scattering lengths $a_{\Sigma^+ n} + a_{\Sigma^0 p} = 0.04 - i3.92$ fm with finite $\Delta_{\Sigma N}$ is significantly different from $a_{\Sigma N} = 1.4 - i4.8$ fm for $\Delta_{\Sigma N} = 0$; $a_{\Sigma N}$ is shifted by approximately ~ 1 fm due to the isospin-breaking effects. In other words, the isospin relation (11) is broken largely.

In this result, the isospin-breaking effects enhance the slopes of the cross section at the threshold of $\Sigma^+ n$ while that at the threshold of $\Sigma^0 p$ are suppressed:

$$a_{\Sigma^+ n} - b_{\Sigma^+ n} = -2.7 - i3.0 \quad \text{fm}, \quad (18)$$

$$a_{\Sigma^0 p} - b_{\Sigma^0 p} = -0.54 - i0.71 \quad \text{fm}. \quad (19)$$

Again, we find large deviation from the isospin relation $a_{\Sigma^+n} - b_{\Sigma^+n} = 2(a_{\Sigma^0p} - b_{\Sigma^0p})$. Consequently, the cusp structure at the Σ^+n threshold is much stronger than that at the Σ^0p threshold. In this way, the large isospin-breaking effects may change the behavior of the cusp structures while the two cusp structures are related in the isospin-symmetric limit.

4. Summary

In this contribution, we study the isospin-breaking effects on threshold cusp structures in coupled-channel hadronic scattering. First, in Sec. 2, we introduce a convenient representation of the scattering amplitude that enables a transparent analysis of the slopes of the cross section near thresholds. Applying this framework to the ΛN - ΣN coupled-channel system, we analyze the cusp structures appearing in Λp elastic scattering in both the isospin-symmetric and isospin-broken cases. We show that, when the isospin-breaking effects are small, the cusp structures at the Σ^+n and Σ^0p thresholds exhibit similar shapes and merge into a single cusp in the isospin-symmetric limit. In Sec. 3, we show two numerical results: one corresponding to the case where the isospin-breaking effects are small, and the other to the case where they are sizable. For larger isospin-breaking, the sharpness of the two cusps differs significantly, reflecting the modifications of the slopes of the cross section induced by the isospin-breaking effects.

Acknowledgments

This work has been supported in part by the Grants-in-Aid for Scientific Research from JSPS (Grants No. JP23H05439, No. JP22K03637, and by JSPS KAKENHI Grant Number 25KJ1996, and by MIYAKO-MIRAI Project of Tokyo Metropolitan University.

References

- [1] A. Esposito, L. Maiani, A. Pilloni, A.D. Polosa and V. Riquer, *From the line shape of the $X(3872)$ to its structure*, *Phys. Rev. D* **105** (2022) L031503 [2108.11413].
- [2] LHCb collaboration, *Study of the doubly charmed tetraquark T_{cc}^+* , *Nature Commun.* **13** (2022) 3351 [2109.01056].
- [3] V. Baru, J. Haidenbauer, C. Hanhart, A.E. Kudryavtsev and U.-G. Meißner, *Flatté-like distributions and the $a_0(980)/f_0(980)$ mesons*, *Eur. Phys. J. A* **23** (2005) 523 [nucl-th/0410099].
- [4] F.-K. Guo, X.-H. Liu and S. Sakai, *Threshold cusps and triangle singularities in hadronic reactions*, *Prog. Part. Nucl. Phys.* **112** (2020) 103757 [1912.07030].
- [5] K. Sone and T. Hyodo, *General amplitude of near-threshold hadron scattering for exotic hadrons*, *Phys. Rev. C* **112** (2025) 065207 [2405.08436].
- [6] K. Sone and T. Hyodo, *Threshold cusp structures in multi-channel scattering*, 7, 2025 [2507.17260].
- [7] PARTICLE DATA GROUP collaboration, *Review of particle physics*, *Phys. Rev. D* **110** (2024) 030001.
- [8] T. Nishibuchi and T. Hyodo, *Analysis of the $\Xi(1620)$ resonance and $\bar{K}\Lambda$ scattering length with a chiral unitary approach*, *Phys. Rev. C* **109** (2024) 015203 [2305.10753].
- [9] J. Haidenbauer, U.G. Meißner and A. Nogga, *Hyperon–nucleon interaction within chiral effective field theory revisited*, *Eur. Phys. J. A* **56** (2020) 91 [1906.11681].
- [10] J. Haidenbauer and U.-G. Meißner, *On the structure in the ΛN cross section at the ΣN threshold*, *Chin. Phys. C* **45** (2021) 094104 [2105.00836].
- [11] J. Haidenbauer, U.-G. Meißner, A. Nogga and H. Le, *Hyperon–nucleon interaction in chiral effective field theory at next-to-next-to-leading order*, *Eur. Phys. J. A* **59** (2023) 63 [2301.00722].